Interlayer bonding in compounds with the $ThCr_2Si_2$-type structure: Insight on the ferromagnetism of $SrCo_2(Ge_{1-x}P_x)_2$ from electronic structure calculations

E. Cuervo-Reyes* and R. Nesper†

Swiss Federal Laboratories of Materials Science and Technology, Überlandstrasse 129, CH-8600 Dübendorf, Switzerland, and Swiss Federal Institute of Technology (ETH), CH-8093 Zürich, Switzerland

(Received 11 February 2014; revised manuscript received 11 May 2014; published 15 August 2014)

The strong composition dependence of the cell parameters in (more than 700) compounds with the $ThCr_2Si_2$-type structure has been the subject of discussion for several decades. Recent findings of ferromagnetism in $SrCo_2[Ge_{1-x}P_x]_2$ with a quantum critical point at $x \approx 0.325$ have revived interest in the composition-property relationship in such systems. In this article, we present a theoretical insight on these phenomena, supported by electronic structure calculations. We discuss the differences between $SrCo_2[Ge_{1-x}P_x]_2$ and related compounds, and we conclude that previous analyses based on the filling of "relevant" molecular orbitals are case specific and do not describe the general mechanism behind the changes in the cell parameters. We propose a more physical reasoning, based on electronic kinetic energy and electron-core interactions, which gives a unified picture of all cases. With respect to the magnetism in $SrCo_2[Ge_{1-x}P_x]_2$, we find that the density of states at the Fermi level and the Curie temperature display very similar dependences on the composition. Our calculations support the classification of the magnetic dome as a weak itinerant ferromagnetism, and they are consistent with the Stoner-enhanced paramagnetism observed in samples with $x > 0.75$. We argue that the interlayer bonding is *metallic* (instead of covalent) from $x = 0$ up to the value at which the magnetic remanence disappears.

DOI: 10.1103/PhysRevB.90.064416 PACS number(s): 75.10.Lp, 71.20.Lp, 71.10.Ca, 82.20.Wt

I. INTRODUCTION

Over 700 compounds, which adopt the body-centered tetragonal $ThCr_2Si_2$-type structure [1–5], have been reported to date. This AT_2X_2 structure consists of puckered transition-metal-metalloid T_2X_2 layers, stacked along the c axis, with main group or lanthanide cations (A) sitting in the voids (see Fig. 1).

Interest in these compounds has regrown in the past decade since they have been found to display a variety of physical phenomena; for instance, non-Fermi-liquid behavior [6] in $YbRh_2Si_2$, unconventional superconductivity [7] in K-doped $BaFe_2As_2$, and several sorts of magnetic ordering. This diversity is to a certain extent related to the tunability of the unit-cell parameters. The 122 compounds occur in an unusually broad range of the lattice-constant ratio (c/a) [8,9]. A general trend is that, for a same cation (A) and a same p element (X), the X-X distance between neighboring layers decreases as T moves from left to right in the periodic table. The description of this effect in terms of a transfer of electrons from antibonding X-X orbitals toward the T-d shell was given by Hoffmann and Zheng in 1985 [8].

The filling of the anionic T_2X_2 bands and their dimensionality can also be controlled by changing the valence of the metalloid and the size of the cation A [10–13]. The solid solution $CaCo_2[Ge_{1-x}P_x]_2$ is considered to be an example with bonded X-X dimers through the whole composition range. With the increase in phosphorus content, electrons are added to the Co d shell, driving the system from nonmagnetic to antiferromagnetic [14,15]. The increase in Sr content in $Ca_{1-x}Sr_xCo_2P_2$ causes the breaking of the P_2 dimers and the loss of the antiferromagnetic order. No magnetic ordering occurs in $BaCo_2[Ge_{1-x}P_x]_2$. The large size of the Ba^{2+} cation hinders the formation of X-X bonds, switching off the magnetic interactions between the layers [16]. It has also been found that the transition from nonbonded to bonded dimers can be induced by applying pressure [17–19].

Recently, Jia *et al.* [20] reported structural and magnetic data of $SrCo_2[Ge_{1-x}P_x]_2$ for several values of x. The authors found that samples with intermediate compositions show itinerant ferromagnetism. For $x < 0.325$ the compounds behave as Pauli paramagnets. The magnetic phase starts at a quantum critical point (QCP) around $x = 0.325$. The critical temperature grows with x, taking its maximum value of $T_C = 35$ K at $x = 0.55$. As x continues to increase, T_C decreases, and the system seems to have a crossover to a Stoner-enhanced paramagnetism around $x = 0.8$. According to the reported magnetic data, the saturation magnetization at $T = 2$ K remains high for $x > 0.75$, but there is no remanence. In parallel to the changes in magnetic behavior as a function of x, the lattice constants were shown to follow a continuous S-shaped change with a significant enlargement of the c axis. The authors postulated that the occurrence of the QCP is not driven by the doping of the cobalt d bands but is related to the breaking of the interlayer X-X bond. They proposed that the extra electrons, introduced with the increase in x, remain on the antibonding p_z states. The gradual filling of this band could create a high density of states (DOS) at the Fermi level (FE) at intermediate compositions, which could surpass the Stoner criterion. As such, the elongation of the cell in $SrCo_2[Ge_{1-x}P_x]_2$ seems to adhere to the mechanism proposed by Hoffmann and Zheng [8]. However, there is no complete consensus on this point [21,22].

From theoretical calculations on the $Ca[Fe_{1-x}Ni_x]_2As_2$ system [22], Pobel and co-workers have suggested that neither the elongation of the c axis, nor the magnetism in $SrCo_2[Ge_{1-x}P_x]_2$ is caused by changes in the valence of the anions. In light of their simulations, the direct X-X covalent

*eduardo.cuervoreyes@empa.ch
†reinhard.nesper@inorg.chem.ethz.ch

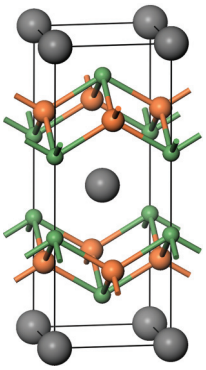

FIG. 1. (Color) The $ThCr_2Si_2$-type structure. $A/T/X$ atoms are shown as gray/orange/green spheres.

interaction is very weak. They found that in $Ca[Fe_{1-x}Ni_x]_2As_2$, there is no change in the total occupation of the As-As states and that the formation of the dimers is related to the weakening of T-T bonds. The strong p-d hybridization causes a splitting of both the $pp\sigma$ and the $pp\sigma^*$ states and an overlap of their energy windows. Similar results were previously reported by Johrendt *et al.* [21] concerning other 122 compounds. Depending on the composition, changes in the electron count can reflect on the occupation of bonding and antibonding states in an unconventional manner, i.e., changes in the overall bonding character without altering the total valence of the anions.

In the present paper, we provide a theoretical insight on the electronic structure and interlayer bonding in $SrCo_2[Ge_{1-x}P_x]_2$, supported by numerical evidence. We present results from first-principles calculations which are in excellent agreement with the magnetic data [20] and allow us to assess previous hypotheses. Our calculations are compatible with the occurrence of a ferromagnetic dome with an itinerant character, triggered by a Stoner instability. Moreover, we find a strikingly high correlation between the x dependence of the critical temperature and that of the DOS at the Fermi level. We find that the ground state of a Co_2P_2 layer is magnetic. This, together with the absence of interlayer bonding, explains the enhanced paramagnetism observed in the experiments. On the subject of changes in the interlayer bonding, we agree with both Jia *et al.* [20] and Pobel *et al.* [22] to a point, but we think that either of their interpretations may be correct within a specific subgroup of compounds, and neither of the two describes the case of $SrCo_2[Ge_{1-x}P_x]_2$ completely. Our simulations confirm that, in $SrCo_2[Ge_{1-x}P_x]_2$, the $2x$ electrons remain at the anions. The variation in the P content does not affect the total occupation of cobalt d states, but it does change their energy distribution through a strong hybridization. The main contribution to the DOS at the Fermi level comes from Co d states. The electron localization function (ELF) does not show evidence of covalent X-X interaction and indicates that the interlayer contact in germanide is metallic. In the pure phosphide, the interlayer contact is ionic. The calculated band structures are consistent with this interpretation. A unified picture of the interlayer bonding in this type of compound does exist, which is also presented in this article.

We have divided the main body of the paper in two sections. In Sec. II we describe the theoretical methods, whereas the main results and discussion are presented in Sec. III. Final remarks are made in Sec. IV. Details of the numerical calculations, which do not necessarily contribute to understanding of the discussion, are given in a separate Appendix.

II. THEORETICAL METHODS

The electronic structures of $SrCo_2Ge_2$ and $SrCo_2P_2$ were calculated using several implementations of the density functional theory (DFT). The codes employed and calculation parameters are described in the Appendix.

We started by verifying whether DFT could provide us with a reasonable approximation to the electronic structure of this system, or if corrections for the Coulomb repulsion would be necessary [23]. To this end, we performed spin-polarized DFT and DFT + U calculations and checked whether the U correction introduced significant changes in the band structure. We found out that the simple DFT results are robust against the U correction. The occupations of the cobalt d orbitals varied in less than 0.1 electrons per atom. We found no evidence of electron localization caused by the on-site repulsion. Since all experimental evidence [20] indicate that the compounds are metallic and their magnetism has itinerant character, we believe that our calculated band structures are qualitatively correct.

We studied the possibility of a ferromagnetic ground state by: (i) calculating the nonpolarized DOS for several values of x and (ii) comparing the total energies of the polarized and nonpolarized solutions.

The electronic structures at intermediate compositions were calculated within the virtual crystal approximation (VCA) [24]. The metallic character and absence of structural distortion or site preference allow us to take Ge and P sites as a generic (X) "average" atom, whose energy levels and valence vary continuously with the composition. The VCA describes well those phenomena that depend on global (self-averaging) quantities, and as such, it may be suitable for the description of the itinerant magnetism in the $SrCo_2[Ge_{1-x}P_x]_2$ solid solution. By construction, quantities that depend on spatial fluctuations, atomic forces, and deviations from the Vagart law are not always well captured by the VCA approximation. For this reason, we took the experimental structural parameters available for each of the compositions.

For a representation of the bonding structure in real space, we employed the ELF [25], implemented by Savin and coworkers [26,27] in the LMTO-ASA code of Andersen and Jepsen [28]. The ELF is a function of the space coordinates (x,y,z). It shows the distribution of localization[1] attractors in real space, and its topology provides useful information of the structural

[1]The term localization in the ELF has a different meaning, and not related to Mott [29–31] or Anderson [31–33] localizations. The last two refer to the gapped mobility of the electrons as a consequence of electron-electron Coulomb repulsion and electrostatic disorder, respectively. The ELF has little to do with disorder or interaction; it is related to the spatial extension and distribution of electronic states and how they contribute to the total density following the Pauli exclusion principle.

bonding. It is defined, for an independent-particle model, as

$$\mathrm{ELF}(\mathbf{r}) = \left[1 + \left(\frac{\tau(\mathbf{r})}{\tau_h(\mathbf{r})}\right)^2\right]^{-1}, \quad (1)$$

where

$$\tau(\mathbf{r}) = \frac{1}{2}\sum_{i=i}^{N} |\nabla\psi_i|^2 - \frac{1}{8}\frac{|\nabla\rho|^2}{\rho} \quad (2)$$

is the excess of kinetic-energy density due to the Pauli exclusion principle and

$$\tau_h(\mathbf{r}) = \tfrac{3}{10}(3\pi^2)^{2/3}\rho^{5/3} \quad (3)$$

is the $\tau(\mathbf{r})$ of a homogeneous electron gas with the density replaced by $\rho(\mathbf{r})$. The sum in Eq. (2) runs over all occupied spin orbitals $\psi_i(\mathbf{r})$, and it is invariant to canonical transformations of the orbitals. Thus, the ELF is independent of the employed basis set. In addition, the ELF has been found to depend very weakly on the theory level (Hartree-Fock, DFT, extended Hückle, etc.) [34,35]. We employ the LMTO-ASA code because (being an all-electron method) it allows us to choose whether we want to compute the true ELF or to intentionally exclude the core states.

Because of the Lorentzian scaling in Eq. (1), the ELF takes continuous values between 0 and 1. For light elements or more generally in regions where only s and p atomic orbitals are necessary for the complete description of the electron density, ELF > 0.75 is a good criterion to identify closed shells, covalent bonds, and lone pairs. Regions with localized states involving higher angular momentum display lower ELF values. However, the topological analysis (distribution of stationary points) remains valid.

A homogeneous free-electron gas will have, by definition, ELF $= 0.5$ everywhere, regardless of its density. This is a structureless system. A physical system may be thought of as setting cores into this sea. This will distort the homogeneous ELF, which will acquire higher values where electrons states localize. It will also take smaller values in the regions between the localization attractors. Regions with low ELF values cannot be interpreted as having electrons more delocalized than the perfectly delocalized homogeneous electron gas. They represent the divisions (walls) between the basins. The weak point in the quantitative description is that the ELF is not additive and does not satisfy a sum rule. Nevertheless, a reasonably extended region with ELF ≈ 0.5 (a region without distortion) can be considered an indication of free-electron gaslike behavior, i.e., metallic bonding. Since the ELF is a continuous function, ELF values close to 0.5 also appear between attractors and walls. These are generally closed surfaces and are not related to free-electron-gas behavior.

For a thorough description of this methodology and representative examples the reader is referred the listed references [26,27,35–38]. The literature on the electron localizability indicator is also recommended; see, for example, Ref. [39].

It is useful to combine the ELF and ρ in the same graph. This allows one to distinguish cores and two center-two electron bonds (where ρ is relatively high) from localization patterns in interstitial regions which could correspond to multicenter bonds or to overlooked anions [35,38]. To this end, we use a code developed in our group, which depicts ρ and ELF values by the density of points and their color, respectively, over a black background. Colors are assigned as in an elevation map, following the sequence: deep blue, blue, cyan, green, yellow, orange, brown, grayish white, and white.

III. RESULTS AND DISCUSSION

A. Dependence on x of the interlayer bonding in $SrCo_2[Ge_{1-x}P_x]_2$

The band structure for each of the parent compounds ($SrCo_2Ge_2$ and $SrCo_2P_2$) are shown in Fig. 2 (left and right panels, respectively). The FE has been taken as zero energy. Both band structures correspond to metallic systems as it should be. For $x = 0$ two nearly degenerate bands cross the Fermi level along the Z direction in reciprocal space, whereas this feature is missing for $x = 1$. Conversely, the number of states around the FE originating from bands running in the other directions is higher for $x = 1$. Therefore, $SrCo_2Ge_2$ is a 3D metal, and $SrCo_2P_2$ is a 2D metal with a higher DOS at the FE. The corresponding partial DOS and the DOS for several intermediate compositions are displayed in Fig. 3 (where only energies from -6 to 1 eV are shown).

The first aspect that becomes evident is the strong mixing of cobalt d with X-p states. Johrendt *et al.* already pointed out [21] that the hybridization of the T-d states with the X-p orbitals can cause a partial inversion or overlap in the energy ranges of the $pp\sigma$ (bonding) and the $pp\sigma^*$ (antibonding) states. As a consequence, there are compositions at which electrons partially occupy the $pp\sigma^*$ before the $pp\sigma$ are completely filled, depending on the relative electronegativities of the elements and atomic sizes. In this way, the partial substitution of any of the elements could change the character of a bonding interaction sometimes without changing the overall effective valence. With all these variables, it may not be possible to describe the structural changes in all compounds in terms of the same single orbital filling mechanism. The analyses presented by Hoffmann and Zheng [8] for the manganese phosphides and by Pobel *et al.* [22] for Fe/Ni arsenides may not completely

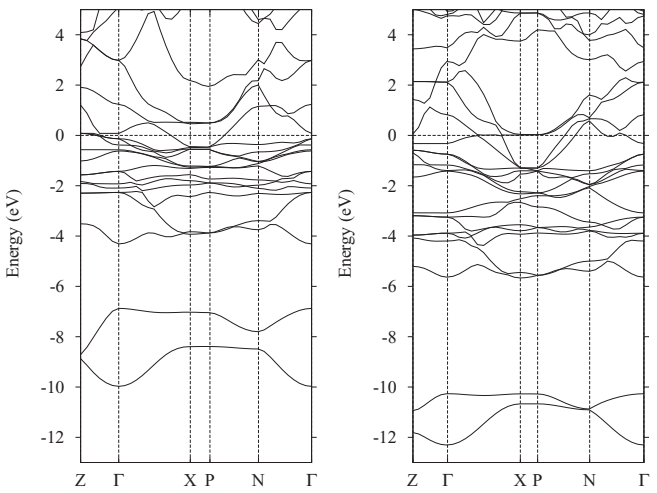

FIG. 2. Band structure of (left) $SrCo_2Ge_2$ and (right) $SrCo_2P_2$. The latter has no band crossing the FE in the Γ-Z segment.

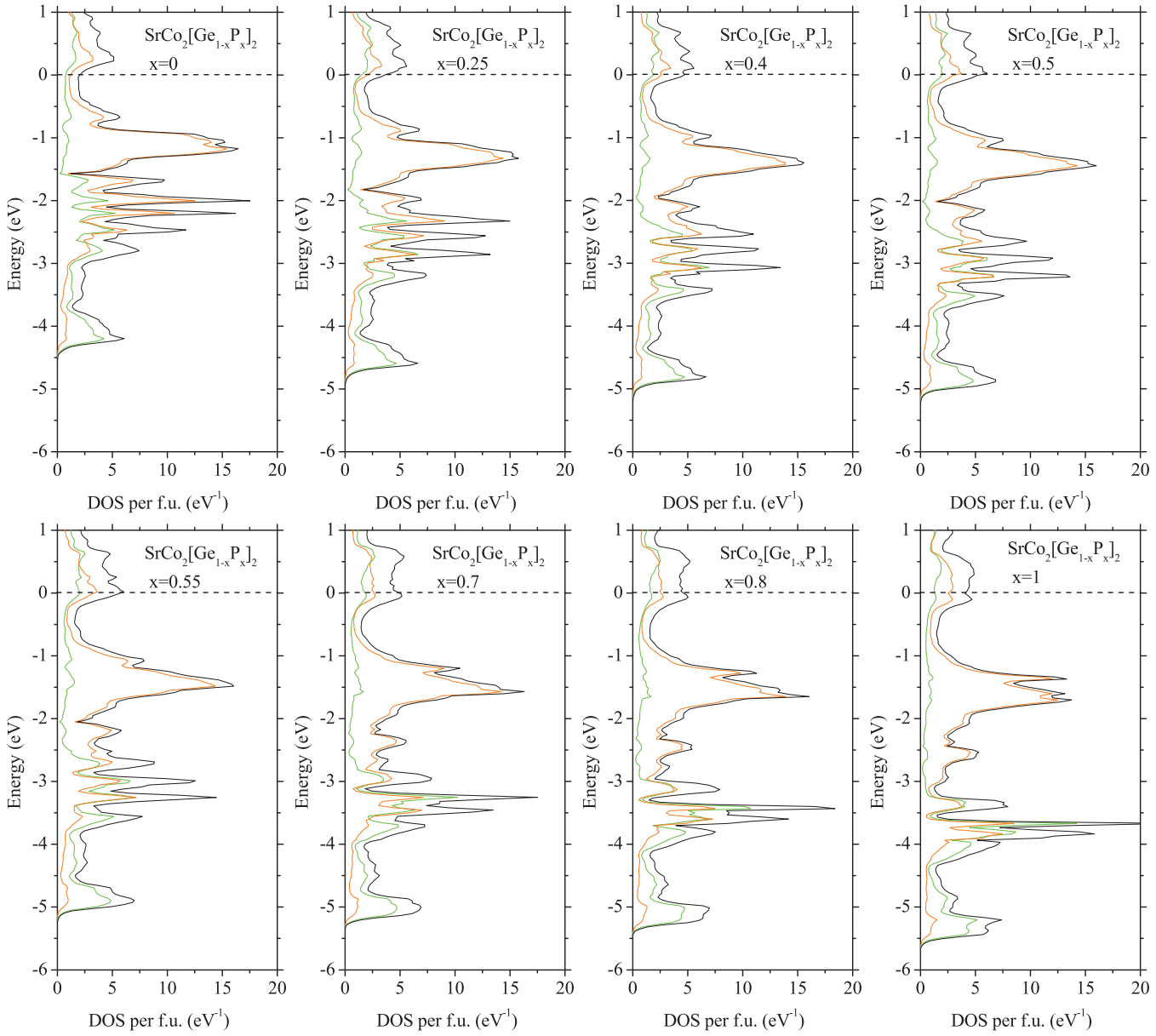

FIG. 3. (Color) The partial density of states per formula unit of $SrCo_2[Ge_{1-x}P_x]_2$ in the virtual crystal approximation for several values of x. The green (orange) line corresponds to p (d) states; the total density of states is shown in black. Ge/P s states are not shown. Formula units are represented by f.u.

represent the situation in $SrCo_2[Ge_{1-x}P_x]_2$. In the following we will show that this is actually the case.

According to the integrated DOS, there is in $SrCo_2P_2$ one more valence electron per X atom than in $SrCo_2Ge_2$. The total population of Co d states is practically unchanged. X-p states are shifted down with respect to Co d states and take the extra electrons. At the same time, following the evolution of the FE from $x = 0$ to $x = 1$, one sees that it crosses a maximum in the DOS at intermediate compositions. So far, this seems to be what Cava and co-workers proposed, and the elongation of the cell seems to follow the filling of the X-X (perhaps) antibonding states. However, the DOS around the FE is dominated by the Co d contribution for any composition. In addition, whether the extra electrons go to the $pp\sigma$ or $pp\sigma^*$ combinations is not essential since the direct overlap of the two p states is very poor. In this context, $pp\sigma$ and $pp\sigma^*$ are just symmetric and antisymmetric combinations of the atomic p orbitals with no special physical relevance since they are energetically similar. In fact, the overlap population analysis gives no direct bonding interaction in the pure phosphide and a weak antibonding interaction in germanide. Note that Pobel *et al.* [22] also found a weak antibonding X-X direct interaction in the 122 calcium Ni/Fe arsenide, despite the smaller size of the calcium cations.

These electronic rearrangements might seem unconventional for one simple reason; we are trying to understand them in terms of atomic orbitals. Atomic orbitals are a mathematical construction which help us to rationalize the bonding of structures in many but not all cases. When the electrons are delocalized, many atomic orbitals are needed for

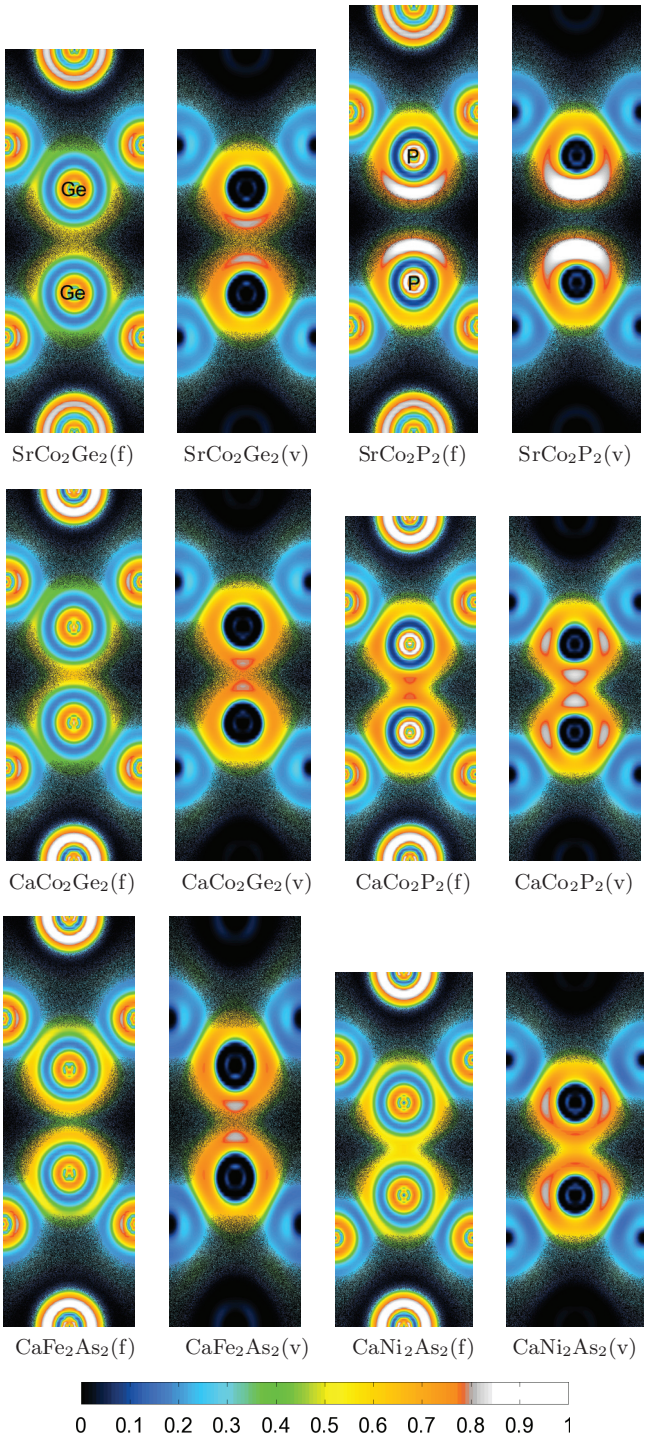

FIG. 4. (Color) $y = 0$ section of the electron localization function of several 122 compounds. (f) denotes full ELF; (v) indicates that only valence states were used.

a complete description of the relevant electronic states, and the interpretation of the bonding in terms of the population analysis is not the most transparent. The structural changes in $SrCo_2[Ge_{1-x}P_x]_2$ can be well understood in more fundamental terms, by looking at the competition between electrostatic and kinetic energies of the electrons.

In general, the electron-core interaction is minimized when the electrons are tightly bound to the most attractive positive center. Conversely, the kinetic energy is reduced when the electrons are spread over larger regions of space. The size of an isolated atom corresponds to the optimal distribution that minimizes the total energy taking the Pauli exclusion principle into account. By delocalizing or sharing electrons among two or more atomic centers, the system may lower the kinetic energy (depending on the competition between uncertainty and exclusion principles) but at the expense of a loss of potential energy. In order not to lose too much electron-core energy, the cores approach each other, resulting in the formation of a compound. These basic ideas can be applied to the interlayer bonding in $SrCo_2[Ge_{1-x}P_x]_2$.

The electronegativity difference between P and Sr is larger than between Ge and Sr. Thus, in the former case the system is better off keeping the electrons more tightly bound to the P centers and setting each pair of anionic layers as far as possible with cations intercalated. The direct coupling between the anions is null or weakly antibonding, and they are held together by the cations. As the content of germanium is increased, the electrons become less attracted by the X cores, and the best way to optimize the energy is by reducing the kinetic component, i.e., delocalizing the charge in between the layers. This however, would represent a big loss in electron-core interaction, which is partially avoided by reducing the interlayer distance. This conclusion is supported by numerical results. We found that the kinetic energy in germanide is higher by 1.35 hartree per formula unit than it would be if the compound would adopt the lattice parameters of the phosphide. The former solution (with a shorter cell) is more stable because it loses less potential energy. The quasi-2D electron confinement in the phosphide is driven by potential energy (higher electronegativity), and the amount of kinetic energy gained with the formation of this compound is lower than in germanide.

Next, we look at the bonding from another base-independent perspective employing the ELF. Planar cuts of the ELF along the dumbbells are shown in Fig. 4. The upper row contains the plots with the full ELF of $SrCo_2Ge_2$, the valence ELF of $SrCo_2Ge_2$, the full ELF of $SrCo_2P_2$, and the valence ELF of $SrCo_2P_2$ from left to right. For a more complete analysis, we also show the respective plots from $CaCo_2Ge_2$ and $CaCo_2P_2$ in the middle row and those from $CaFe_2As_2$ and $CaNi_2As_2$ in the lower row. The size ratios of the frames are the same as those of the actual unit cells. We also present the ELF calculated without core states in order to highlight base-dependent features, such as the direct interaction of atomic valence states. Regions with strong contributions from d states show, as mentioned in the previous section, low ELF values (see, for example, the regions occupied by cobalt). However, this does not affect the direct X-X contact.

The contact between the germanium atoms in $SrCo_2Ge_2$ does not show a maximum in the middle of the dumbbell. In contrast, it shows a spread (and rather flat in values) green-yellow region. The shape of the ELF in single-bonded dumbbells with four cations around its waist is well known. A covalent bond would show up as a single localization attractor

halfway in between the cores, which is clearly not present in this case. This, together with a band crossing the Fermi level in the Γ-Z segment with a contribution of p_z states, is all indicative of a metallic bonding. In the phosphide, there is no bonding at all. The ELF shows two strong attractors (the lone pairs, one per phosphorus atom) facing each other, separated by an avoided region. In the plots without cores, one sees that these two attractors (that correspond to a nonbonding direct p-p interaction) have already started to develop in germanide, surrounded by the metallic cloud. Remember that we also found a net Ge-Ge antibonding interaction in the overlap population analysis.

We found it interesting to present the ELFs of $CaCo_2Ge_2$ and $CaCo_2P_2$ because, despite the smaller size of the Ca cation and the shorter interlayer distance, there is no X-X covalent bonding either. The interaction is metallic in both cases, and both feature two small localization attractors opposing each other. The localization regions are more developed in the phosphide than in germanide (which is due to the higher electronegativity of the former), but there is no qualitative difference in the X-X contact. In both cases, the ELF at the center of the dumbbell displays a (rather flat) saddle point (minimum along the dumbbell axis and maximum in the perpendicular plane). In comparison with the strontium compounds, the smaller size of Ca favors the metallic character of the interlayer contact.

The case of the iron nickel arsenide is also nicely illustrated by means of the ELF. Here we have the same X element (As) in both Fe and Ni compounds. Whereas the overall level of localization around the anions remains nearly constant, the arrangement of the attractors does change. In the iron compound, one has almost separated shells with slightly developed lone pairs opposing each other. In the nickel compound, the attractors have been shifted to in-plane directions, and the shells are fused together. As such, the ELF represents the improvement of the interlayer metallic bonding at the expense of a change in the intralayer bonding. The changes in the T-As interaction causes a distortion of the As shell without a change in its total charge.

The above examples show that the information contained in the ELF is consistent with the interpretation of Pobel *et al.* [22] of the calcium Fe/Ni arsenides, and they also confirm that the structural changes in $SrCo_2[Ge_{1-x}P_x]_2$ cannot be related to the same orbital filling mechanism. The electronic rearrangement in $CaCo_2[Ge_{1-x}P_x]_2$ also follows a slightly different route. There is not a one-to-one correspondence between the changes in the filling of a given orbital and the structural changes in all compounds. The mechanisms proposed in Refs. [8,20–22], which are based on the changes in the bonding interaction of a pair of orbitals, may be adequate within a particular set of compounds but fail when applied to a different system. However, a unified picture does exist, which allows us to understand the composition dependence of the unit-cell length in most 122 compounds. The idea is to look at the electronic behavior at a fundamental level without introducing arbitrary orbitals.

This general situation can be represented in a very simplified manner by an electron gas in the presence of a periodic potential. Figure 5 shows the sketches of the two common situations (a) a unit cell with ionic interlayer contact and (b) a unit cell with metallic contact. The solid line represents $V(z)$, a simplification of the effective electrostatic potential. The horizontal dashed line is the Fermi level, and the area below represents the sea of electrons. The exact functional form of $V(z)$ is not essential; the important feature is the alternating arrangement of high and low potential regions, corresponding to the cationic (A) and anionic (T_2X_2) layers, respectively. Whether the system is metallic or ionic depends on three variables: potential depth, potential width, and number of electrons. The dependence of the electronic states on these parameters is well understood from fundamental physics. The delocalization of the electrons along z can be controlled with any of the three fundamental variables. One route is by reducing the cation size with no or some decrease in the electronegativity difference. This corresponds, for instance, to the $Ca_xSr_{1-x}Co_2P_2$ system. Another route is the increase in the electron number with little changes in electronegativity and size. This is the situation in the $Ca[Fe_{1-x}Ni_x]_2As_2$ solid solution. The transformation in $SrCo_2[Ge_{1-x}P_x]_2$ (from $x = 1$ to $x = 0$) is due to the significant decrease in electronegativity difference, despite the subtraction of two electrons per layer. The delocalization of the electrons always implies a loss of potential energy. This can only happen if the area of the potential barrier ($\sim$height $\times$ width) is small enough in comparison to the gain in kinetic energy.

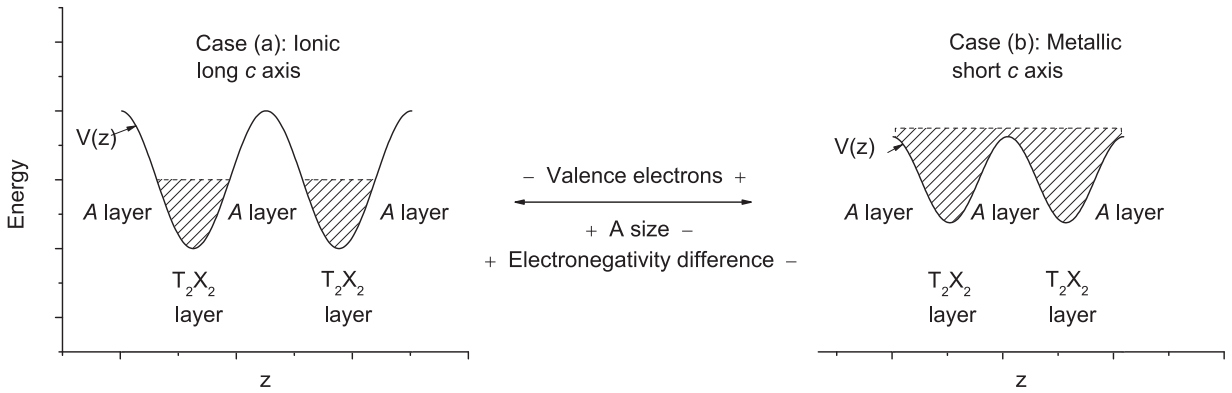

FIG. 5. Sketches of the electronic filling with respect to the effective electrostatic potential along the z axis. Case (a) represents the compounds with ionic interlayer contact; case (b) represents systems with metallic-bonded layers.

B. About the ferromagnetism in $SrCo_2[Ge_{1-x}P_x]_2$

With $x = 1$, the magnetic states of different layers are uncorrelated due to the lack of bonding. We found that solutions with polarized layers have lower energy than the solution with zero-spin density everywhere. The lack of remanence and the enhanced (para)magnetic response can be understood as follows. A spin system with continuous symmetry cannot order at finite temperatures in a dimension lower than D = 3 [40–42]. If there are magnetic anisotropies, the continuous rotational symmetry is broken, and there can be some sort of (quasi)long-range magnetic order along the layers. However, different layers can have different orientations in the absence of a bias field, giving zero macroscopic magnetization. Therefore, there is no remanence in either of the cases. An external magnetic field constitutes a magnetic anisotropy and helps the spins of all layers to point in the same direction. This induced anisotropy in cooperation with the intralayer couplings causes the enhanced nonlinear magnetization curve observed at compositions above $x = 0.75$.

At the opposite end of the composition range ($x = 0$), our calculations predict a nonmagnetic ground state. This is consistent with the Pauli paramagnetism observed by Jia *et al.* [20]. The behavior of the DOS at the FE, shown in Fig. 6, is also compatible with this.

According to the mean-field model for itinerant ferromagnetism, the ground state should be ferromagnetic when the system satisfies the Stoner criterion $gU > 1$. g is the DOS per magnetic atom at the FE in the nonpolarized solution, and U is the effective on-site Coulomb repulsion. U is on the order of 1 eV for late $3d$ transition metals, and the hybridization with the ligands may further reduce this effective value. From first-principles calculations, we find that $g \approx 2\ \mathrm{eV}^{-1}$ at the critical point ($x = 0.325$). Because of the approximated character of both the DFT and the Stoner criterion and due to our limited knowledge about U, it is not prudent to take the calculated values as an absolute truth. However, it is very satisfying that g follows the behavior of T_C very closely, which is precisely what one expects from a weak itinerant ferromagnetism, i.e., T_C is an increasing function of $Ug - 1$. In Fig. 6, one also sees that g remains above the critical value up to $x = 1$. This is consistent with the results from spin-polarized calculations and supports the previously discussed hypothesis on the origin of the enhanced paramagnetism in samples with x close to 1.

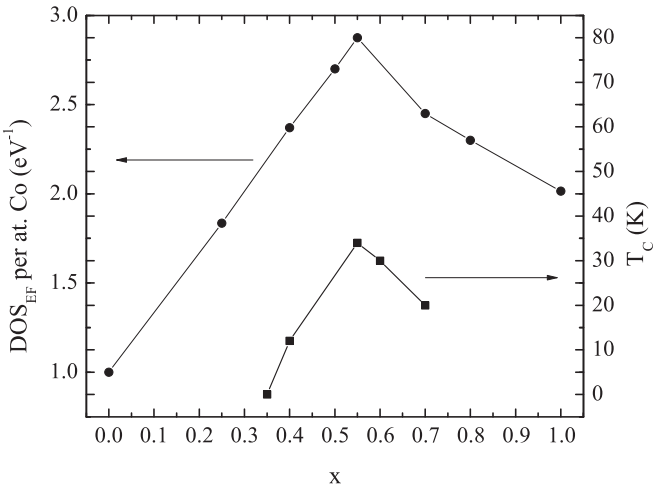

FIG. 6. Density of states of $SrCo_2[Ge_{1-x}P_x]_2$ at the Fermi level for selected values of x, obtained in this paper within the virtual crystal approximation, and critical temperature (T_C) for some compositions reported by Jia *et al.* [20]. The solid lines are a guide to the eye.

IV. CONCLUSIONS

With this paper, we have been able to explain the connection between properties and structural changes in the solid solution $SrCo_2[Ge_{1-x}P_x]_2$. We employed first-principles electronic structure calculations and the electron localization function. This is one example where nontrivial changes in physical properties are explained with an approximated theory of weakly interacting particles. The onset of Stoner ferromagnetism at intermediate compositions was found to be consistent with the changes in the calculated density of states. The electronic redistribution due to changes in the P/Ge ratio also gave a good account of the modifications in the interlayer bonding. We have been able to assess previous hypotheses on the mechanisms behind the surprising behavior of $SrCo_2[Ge_{1-x}P_x]_2$ and its differences with other compounds with the same $ThCr_2Si_2$ structure type. Last but not least, we provided a fundamental explanation for the relation between cell length and composition, which solves the disagreement among previous proposed mechanisms.

ACKNOWLEDGMENTS

This work has been supported by the Swiss National Science Foundation through Grant No. 2-77937-10. The authors thank F. von Rohr for the valuable experimental information provided and the enlightening discussions on the subject. We also thank A. Savin for the insight into old ELF visualization methods and O. Jepsen for the LMTO code.

APPENDIX: CALCULATION SETTINGS

The density of states reported in this paper were extracted from the electronic structure calculations with the CASTEP [43] package in Materials Studio. These were run with the following settings: Perdew-Burke-Ernzerhof exchange-correlation functional [44], norm-conserving pseudopotentials, plane-wave cutoff at 660 eV, $7 \times 7 \times 9$ **k** points, and self-consistency energy tolerance of 5×10^{-7} eV per atom.

For the parent compounds ($x = 0$ and $x = 1$) where the VCA approximation is not needed, we also compared the CASTEP results with DMOL^3 [45]. The latter is computationally more economic for a majority of cases, allowing calculation with a higher density of **k** points to be performed at a lower cost. The DMOL^3 calculations were run treating all electrons on an equal basis (i.e., no pseudopotentials) and were performed on a grid of $17 \times 17 \times 23$ **k** points. Band structures obtained with this method were practically indistinguishable from those performed with CASTEP.

The electron localization function was calculated employing the LMTO code with the following settings: Langreth-Mehl exchange-correlation functional [46],

$8 \times 8 \times 16$ **k** points and Wigner-Seit radii $R(\mathrm{Sr}) = 4.054$, $R(\mathrm{Co}) = 2.346$, and $R(\mathrm{P}) = 2.439$ a.u. (for $SrCo_2P_2$) and $R(\mathrm{Sr}) = 4.280$, $R(\mathrm{Co}) = 2.464$, and $R(\mathrm{Ge}) = 2.583$ a.u. (for $SrCo_2Ge_2$).

[1] Z. Ban and M. Sirika, Acta Crystallogr. **18**, 594 (1965).
[2] R. Marchand and W. Jeitschko, J. Solid State Chem. **24**, 351 (1978).
[3] W. Jeitschko and B. Jaberg, J. Solid State Chem. **35**, 312 (1980).
[4] R. Hoffmann and W. Jeitschko, J. Solid State Chem. **51**, 152 (1984).
[5] W. B. Pearson, J. Solid State Chem. **56**, 278 (1985).
[6] J. Custer, Nature (London) **424**, 524 (2003).
[7] M. Rotter, M. Tegel, and D. Johrendt, Phys. Rev. Lett. **101**, 107006 (2008).
[8] R. Hoffmann and C. Zheng, J. Phys. Chem. **89**, 4175 (1985).
[9] G. Just and P. Paufler, J. Alloys Compd. **232**, 1 (1996).
[10] S. Jia, A. J. Williams, P. W. Stephens, and R. J. Cava, Phys. Rev. B **80**, 165107 (2009).
[11] J. G. Analytis, C. M. J. Andrew, A. I. Coldea, A. McCollam, J.-H. Chu, R. D. McDonald, I. R. Fisher, and A. Carrington, Phys. Rev. Lett. **103**, 076401 (2009).
[12] A. I. Coldea, C. M. J. Andrew, J. G. Analytis, R .D. McDonald, A. F. Bangura, J.-H. Chu, I. R. Fisher, and A. Carrington, Phys. Rev. Lett. **103**, 026404 (2009).
[13] T. Yildirim, Phys. Rev. Lett. **102**, 037003 (2009).
[14] M. Reehuis, W. Jeitschko, G. Kotzyba, B. Zimmer, and X. Hu, J. Alloys. Compd. **266**, 54 (1988).
[15] M. Reehuism and W. Jeitschko, J. Chem. Phys. Solids **51**, 961 (1990).
[16] L. Siggelkow, V. Hlukhyy, and T. F. Fässler, Z. Anorg. Allg. Chem. **636**, 378 (2010).
[17] M. Chefki, M. M. Abd-Elmeguid, H. Micklitz, C. Huhnt, W. Schlabitz, M. Reehuis, and W. Jeitschko, Phys. Rev. Lett. **80**, 802 (1998).
[18] P. C. Canfield *et al.*, Physica C **469**, 404 (2009).
[19] D. Kasinathan, M. Schmitt, K. Koepernik, A. Ormeci, K. Meier, U. Schwarz, M. Hanfland, C. Geibel, Y. Grin, A. Leithe-Jasper, and H. Rosner, Phys. Rev. B **84**, 054509 (2011).
[20] S. Jia, P. Jiramongkolchai, M. R. Suchomel, B. H. Toby, J. G. Chegelsky, N. P. Ong, and R. J. Cava, Nat. Phys. **7**, 207 (2011).
[21] D. Johrendt, C. Felser, O. Jepsen, O. K. Andersen, A. Mewis, and J. Rouxel, J. Solid State Chem. **130**, 254 (1997).
[22] R. Pobel, R. Frankovsky, and D. Johrendt, Z. Naturforsch., B: J. Chem. Sci. **68**, 581 (2013).
[23] M. Imada, A. Fujimory, and Y. Tokura, Rev. Mod. Phys. **70**, 1039 (1998), and references therein.
[24] L. Bellaiche and D. Vanderbilt, Phys. Rev. B **61**, 7877 (2000).
[25] A. D. Becke and K. E. Edgecombe, J. Chem. Phys. **92**, 5397 (1990).
[26] A. Savin, O. Jepsen, J. Flad, O. K. Andersen, H. Preuss, and H. G. von Schnering, Angew. Chem., Int. Ed. Engl. **31**, 187 (1992).
[27] A. Savin, A. D. Becke, J. Flad, R. Nesper, H. Preuss, and H. G. von Schnering, Angew. Chem., Int. Ed. Engl. **30**, 409 (1991).
[28] O. K. Andersen, Phys. Rev. B **12**, 3060 (1975); O. K. Andersen and O. Jepsen, Phys. Rev. Lett. **53**, 2571 (1984); O. K. Andersen, Z. Pawlowska, and O. Jepsen, Phys. Rev. B **34**, 5253 (1986); H. J. Nowak, O. K. Andersen, T. Fujiwara, O. Jepsen, and P. Vargas, *ibid.* **44**, 3577 (1991); W. R. L. Lambrecht and O. K. Andersen, *ibid.* **34**, 2439 (1986); O. Jepsen, O. K. Andersen, and A. R. Machintosh, *ibid.* **12**, 3084 (1975); O. Jepsen and O. K. Andersen, *ibid.* **29**, 5965 (1984); P. E. Blöchl, O. Jepsen, and O. K. Andersen, *ibid.* **49**, 16223 (1994).
[29] N. F. Mott, Proc. Phys. Soc., London, Sect. A **62**, 416 (1949).
[30] N. F. Mott, Rev. Mod. Phys. **40**, 677 (1968).
[31] K. Byczuk, W. Hofstetter, and D. Vollhardt, Phys. Rev. Lett. **94**, 056404 (2005).
[32] P. W. Anderson, Phys. Rev. **109**, 1492 (1958).
[33] E. Abrahams, P. W. Anderson, D. C. Licciardello, and T. V. Ramakrishnan, Phys. Rev. Lett. **42**, 673 (1979).
[34] A. Savin, J. Mol. Struct.: THEOCHEM **727**, 127 (2005).
[35] A. Savin, R. Nesper, S. Wengert, and T. F. Fässler, Angew. Chem., Int. Ed. Engl. **36**, 1808 (1997).
[36] B. Silvi and A. Savin, Nature (London) **371**, 683 (1994).
[37] A very informative review of the ELF and applications as well as a very complete list of references can be found at the web page http://www.cpfs.mpg.de/ELF/ of the Max Planck Institute for Chemical Physics of Solids.
[38] R. Nesper and S. Wengert, Chem.-Eur. J. **3**, 985 (1997).
[39] F. R. Wagner, V. Bezugly, M. Kohout, and Y. Grin, Chem. Eur. J. **13**, 5724 (2007).
[40] N. D. Mermin and H. Wagner, Phys. Rev. Lett. **17**, 1133 (1966).
[41] P. C. Hohenberg, Phys. Rev. **158**, 383 (1967).
[42] S. Coleman, Commun. Math. Phys. **31**, 259 (1973).
[43] S. J. Clark, M. D. Segall, C. J. Pickard, P. J. Hasnip, M. I. J. Probert, K. Refson, and M. C. Payne, Z. Kristallogr. **220**, 567 (2005).
[44] J. P. Perdew, K. Burke, and M. Ernzerhof, Phys. Rev. Lett. **77**, 3865 (1996).
[45] B. Delley, J. Chem. Phys. **113**, 7756 (2000).
[46] D. C. Langreth and M. J. Mehl, Phys. Rev. Lett. **47**, 446 (1981).